Conduction Properties of a New Two-Dimensional Sliding Charge-Density Wave

H.-W. Jiang and A. J. Dahm
Physics Department, Case Western Reserve University, Cleveland, Ohio 44106
(Received 28 November 1988)

The conduction properties of a two-dimensional array of electrons on a helium film supported by a dielectric substrate are reported. The system undergoes a metal-insulator transition at the melting point as substrate imperfections pin the lattice phase. The frequency and field dependence of the finite-frequency conductivity and the noise characteristics are analogous to those of sliding charge-density waves.

PACS numbers: 71.45.Lr, 71.30.+h, 72.70.+m, 73.20.Dx

Some transition-metal trichalcogenides undergo a Peierls transition resulting in a charge-density wave. The pinning and dynamics of such charge-density waves have attracted considerable experimental and theoretical interest.[1] We report here the conduction properties of a new and analogous system: a two-dimensional electron lattice supported by a helium film adsorbed on a dielectric substrate. These properties are reminiscent of those of sliding charge-density waves (SCDW). With a better characterization of the substrate potentials or prefabricated substrate potentials, this system could be a model system for the study of SCDW.

Substrate roughness, which causes a spatial variation of the image potential of the electrons, is the cause of an "impurity" potential which traps electrons. The lattice phase is pinned by these impurity traps, and, thus, the electron layer undergoes a metal-insulator transition at the melting point. This system differs from other charge-density waves in that it is a two-dimensional, classical system; it does not result from a lattice distortion; charge-density-wave conduction is the only current source; and it is dominated by Coulomb interactions. The effect of Coulomb interactions should play an important role in the conduction properties. A classical system has the advantage of eliminating certain models in interpreting the data. Furthermore, it has the advantage that both the charge-density wavelength, i.e., the electron density, and the impurity potentials can be varied, *in situ*. The potentials are varied by changing the film thickness.

Our experimental cell and technique have been described elsewhere.[2] A Fisher brand cover glass with thickness of 160 μm and dielectric constant $\epsilon=7.3$ is used as our substrate. The roughness profile of the slide is scanned by a DektakII spectrometer with 1-μm-diam tip. The traces show a peak-to-peak roughness of about 20 Å with a typical wavelength of 3–5 μm. Two 10×10-mm^2 electrodes are evaporated on the underside of the slide, and a 2-mm-wide guard electrode surrounds these electrodes. The Sommer method[3] is used to measure the impedance of the electron layer with an alternating current. Surface electrons are capacitively coupled to excitation and detection electrodes through the substrate and helium film. The real and imaginary parts of the impedance of the cell are measured to determine the resistivity ρ and the series reactance per square, r, of the electron layer, respectively. Further details, including a determination of the film thickness and electron density will be described in a future publication.

There are two considerations which may be important in an interpretation of the experimental results. With our design, the current and electric field profiles along the current direction are nonuniform. The current is a maximum in the center of the sample and vanishes at the edges. Secondly, the effective mass of the electrons in the crystal phase is enhanced by a small depression in the helium surface which forms under each localized electron.[4] This is a result of applied and image electric fields E directed normal to the surface. These depressions move with the electrons at low velocities. The hydrodynamic mass is proportional to $E^2n^{-1/2}$ and is $\simeq10^4$ times the bare mass at an areal density n of 5×10^9 cm^{-2} and a film thickness t of 300 Å.

Figure 1 shows typical traces of the electron resistivity as a function of temperature at a probing frequency,

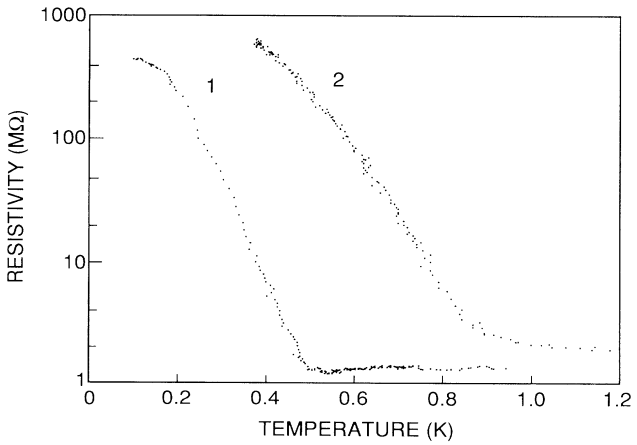

FIG. 1. Resistivity vs temperature for two samples: (1) $n=2\times10^9$ cm, $t=380$ Å; (2) $n=4\times10^9$ cm^{-2}, $t=340$ Å. The excitation frequency and voltage were 100 Hz and 2 mV, respectively.

$\omega/2\pi$, of 100 Hz. In the electron fluid phase, ρ is due to single electron scattering from ripplons and is nearly independent of the temperature as long as the density of helium atoms in the vapor is small, and r is too small to detect. Both ρ and r increase rapidly below a temperature T_c defined by the intersection of extrapolations of the values of $\ln\rho$ in the fluid and solid phases. The transitions in ρ and r sharpen as the probing frequency is reduced. Below T_c, the resistivity can be fitted empirically over a wide temperature range by the relation $\rho=\rho_0 \times\exp(-\gamma T/T_c)$. Here γ is a function of excitation field, excitation frequency, and film thickness, and increases as these parameters are reduced. We attach no physical significance to this particular empirical fit. The reactance per square has the same qualitative behavior with the same value of T_c, but is not fitted by an exponential temperature dependence as well. Large values of resistivity, $\omega\rho/2\pi > 2\times10^4$ MΩ/sec, are less reliable due to a reduced signal-to-noise ratio.

The experimental film thickness was varied from 150 to 600 Å while the electron density was varied from 2×10^8 to $2\times10^{10}/\text{cm}^2$. Within this experimental range, all results follow the above pattern with the transition occurring at the value predicted by the Kosterlitz-Thouless melting theory[5] to within the uncertainty in the screening of the electron-electron interaction. This uncertainty results from an uncertainty in the film thickness.

We interpret the sharp changes in the parameters ρ and r to signal the transition to the crystal phase. Anderson localization as an explanation of this transition can be ruled out by the following observations. For a fixed density, the melting temperature decreases as the film thickness is decreased. This is a result of the enhanced screening of the Coulomb interaction by the substrate.[6] On the other hand, localization effects would occur at a higher temperature as the substrate potential is increased. The transition temperature increases with density for a fixed film thickness as expected for the melting temperature. The nearest-neighbor screened Coulomb interaction potential is $V_{sc}\sim100$ K, while the variation in the substrate image potential V_i is estimated to be ~5 K. Computer simulations[7] show an ordered lattice for $V_{sc}/V_i > 8$, Anderson localization for $V_{sc}/V_i < 10^{-1}$, and an electron glass for intermediate values.

In an uncorrelated fluid the current is carried by free electrons with a mobility limited by scattering from surface ripplons. Below the melting transition we have a lattice pinned by impurity traps. The conduction properties of the pinned lattice are of particular interest and should be analogous to those of one-dimensional sliding charge-density waves in transition-metal trichalcogenides.[1]

The sharp break in the $\ln\rho$ vs T curve gives a well-defined value of T_c. We realize that this may not be identical with the melting point. A gradual variation of ρ near T_c is evident in a plot of ρ vs T shown in the inset of Fig. 2. An enhancement of the resistivity would be expected in a hexatic phase which might separate the liquid and solid phases.[5] This results from correlations between the coordinates of electrons trapped on impurity sites and other electrons. In this case, T_c would represent an upper bound on the melting temperature.

The dominant properties of SCDW are a field- and frequency-dependent conductivity and a large broadband current noise. We report a study of these properties in our system. Our results on a given substrate are completely reproducible. The nonuniform current distribution over the sample prevents us from detecting a narrow-band component of the noise, proportional to the electron velocity as observed in SCDW.

The resistivity of one of our samples is plotted as a function of the rms applied voltage in Fig. 2. The excitation frequency is 10^3 Hz, and the electric field is V/l, where $l\sim1$ cm. The resistivity as a function of temperature for different excitation voltages is shown in the inset for another sample. The resistivity is independent of field below a threshold field E_c which is $\simeq5$ mV/cm for this sample. The value of E_c is frequency dependent at higher frequencies. Both of the parameters ρ and r increase with decreasing film thickness, i.e., increasing trapping potential. The electrons are strongly coupled to excitations in the helium film which acts as a thermal bath. We estimate the electron temperature increase due to Joule heating to be ~1 μK. Thus, heating is not responsible for this field dependence.

Fukuyama and Lee[8] examined the pinning and conductivity of a two-dimensional charge-density wave. The presence of pinning potentials destroys the long-range coherence of the lattice. In the weak-coupling limit they

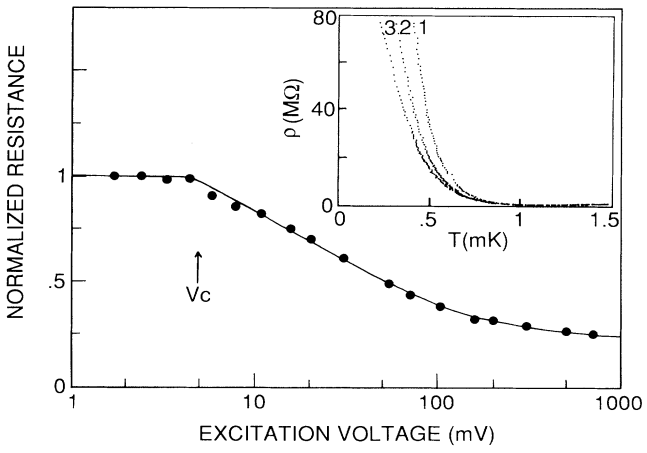

FIG. 2. Resistivity normalized to 7.3 MΩ vs excitation voltage. The experimental parameters were $n=5\times10^9$ cm^{-2}, $t=320$ Å, $f=1$ kHz, and $T=690$ mK. Inset: Resistivity vs temperature for three excitation voltages, (1) 19 mV, (2) 28 mV, and (3) 37 mV.

find the charge-density wave to have phase coherence over a domain of area λ^2. In the absence of an applied field the dominant contributions to the energy of a domain for our system are the long-range Coulomb and impurity energies. We crudely approximate our screened electron-electron interaction by a dipole interaction, $(2et)^2/r^3$. This underestimates the interparticle force. The energy density is given by

$$u = 4ne^2t^2/\pi a\lambda^2 - Wn_i^{1/2}/\lambda ,$$

where a is the lattice spacing, W is the impurity potential, and n_i is the density of impurities. The coherence length λ is obtained by minimizing the energy with respect to the coherence length. The threshold field is estimated by setting the energy gained by the lattice in moving a lattice spacing equal to the cost in impurity energy.[9] This yields

$$E_c \simeq e(2t/a)^2/\lambda^2 \simeq e/\lambda^2 .$$

A typical value of λ for our samples is $\sim 10^3 a$. The ratio λ/a is an order of magnitude larger than in other materials. It is an indication of very weak pinning and results from the large Coulomb interaction. This large value of λ is evidence that the state below T_c is not a Wigner glass.

The field dependence shown in Fig. 2 is characteristic of the behavior of SCDW.[10] For small fields the lattice is pinned by the substrate potentials. At finite frequency, the domains of constant phase polarize and the conductivity is finite. At a threshold field the tilting of the electron potential, applied field plus pinning potential, allows the lattice to slide along the film. The depinning rate increases with applied field until at high fields the entire lattice is completely depinned. Here ripplon scattering limits the mobility of the lattice.[11] The reactance is related to the restoring forces provided by the traps.

The frequency dependences of the resistivity and the reactance per square are shown in Fig. 3. At low frequencies these quantities vary as ω^{-s}. For the resistivity data shown in Fig. 3, the value of s varies from 0.63 to 0.46 as the temperature is raised from 425 to 710 mK. The conductivity is nonlinear, and the Kramers-Kronig relation, which would require the ratio r/ρ to equal the value $\tan(s\pi/2)$, is not applicable. This low-frequency dependence is similar to that observed in the charge-density-wave state[12] of TaS_3. The ω^s conductivity suggests that the collective modes are gapless.

Finally, we examined the statistical fluctuations of the pinning force by measuring the noise spectrum of the current. A large enhancement of the noise is observed in the lattice phase with a $f^{-\alpha}$ spectrum. This is shown in Fig. 4. The value of α is 1.4 ± 0.1, and the values of α observed on different samples range from 0.8 to 1.4. The noise for the same value of resistivity in the fluid phase at high helium vapor densities was instrumental.

We observe a striking, feature of the broadband noise spectrum which is shown in the inset of Fig. 4. At a crit-

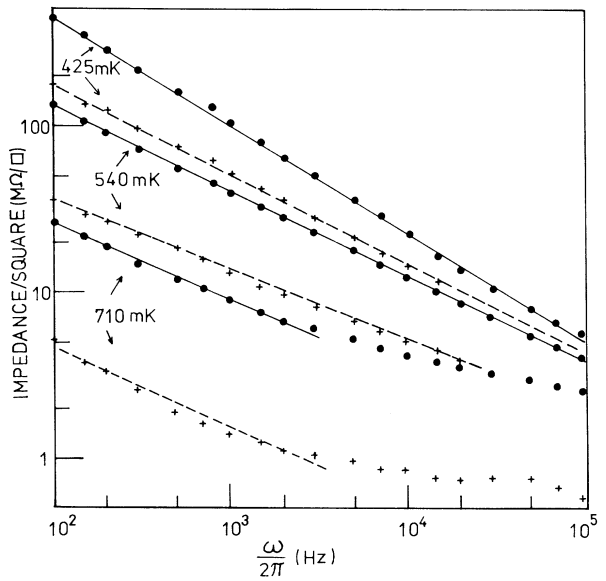

FIG. 3. Real and imaginary parts of the impedance per square vs excitation frequency for three temperatures: ●, resistivity; +, reactance per square. The experimental parameters are $n = 3.8 \times 10^9$ cm^{-2}, $t = 340$ Å, and $V = 20$ mV. The lines are guides to the eye.

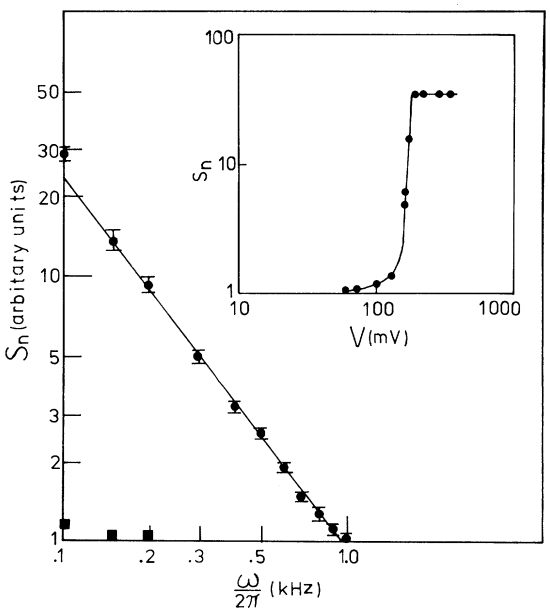

FIG. 4. Noise amplitude S_n vs frequency. The experimental parameters are $n = 10^{10}$ cm^{-2}, $t = 240$ Å, $T = 200$ mK, and $V = 35$ mV. The filled squares represent the instrumental noise. Inset: Broadband noise amplitude S_n vs excitation voltage: $n = 5 \times 10^9$ cm^{-2}, $t = 320$ Å, $T = 50$ mK, and $f = 1$ kHz.

ical value of applied field E_N the amplitude of white noise increases dramatically. The critical field E_N is much greater than E_c and approximately equal to the field at which the conductivity approaches its high-field value (see Fig. 2). Similar behavior has been observed[10] in $NbSe_3$.

As with other SCDW, our results are not explained quantitatively. The detailed nature of our impurity potentials are not known. We expect a random distribution of the depth and possibly the range of the wells. Such a distribution would alter the field and frequency dependence of the resistivity from the predictions of simple models.[13]

In conclusion, we have observed a new metal-insulator transition induced by crystallization of the electrons. The finite-frequency conduction and noise properties are analogous to those of sliding charge-density waves. Since there is no band structure associated with our electron lattice, this implies that these properties in other materials are largely independent of the band structure. Our system is two dimensional, and the Coulomb interaction plays a larger role than in previously reported SCDW. In particular, it leads to a large domain size. The charge-density wavelength and impurity potentials can be varied, *in situ*. In this system, it may be possible to span the spectrum of electronic conduction properties from a freely floating Wigner crystal to a sliding charge-density wave to an electron glass to Anderson localization by varying the film thickness. It may also be possible to fabricate predetermined impurity potentials beginning with a very smooth substrate.

We would like to express our gratitude to M. Saitoh and P. M. Platzman for helpful discussions. This work is supported by the National Science Foundation under Grant No. DMR-87-13922.

[1]For a review of charge-density-wave conduction, see G. Gruner and A. Zettl, Phys. Rep. **119**, 117 (1985).

[2]R. Mehrotra, B. M. Guenin, and A. J. Dahm, Phys. Rev. Lett. **48**, 641 (1982).

[3]R. Mehrotra and A. J. Dahm, J. Low Temp. Phys. **67**, 115 (1987).

[4]D. S. Fisher, B. I. Halperin, and P. M. Platzman, Phys. Rev. Lett. **42**, 798 (1979).

[5]For a review of Kosterlitz-Thouless melting, see K. J. Strandburg, Rev. Mod. Phys. **60**, 161 (1988).

[6]F. M. Peeters and P. M. Platzman, Phys. Rev. Lett. **50**, 2021 (1983).

[7]A. Aoki, J. Phys. C **12**, 633 (1979).

[8]H. Fukuyama and P. A. Lee, Phys. Rev. B **17**, 535 (1978).

[9]P. H. Lee and T. M. Rice, Phys. Rev. B **19**, 3970 (1979).

[10]J. Richard, P. Monceau, M. Papoular, and M. Renard, J. Phys. C **15**, 7157 (1982).

[11]A. J. Dahm and R. Mehrotra, J. Low Temp. Phys. **50**, 201 (1983).

[12]W.-Y. Wu, L. Mihaly, G. Mozurkewich, and G. Gruner, Phys. Rev. Lett. **52**, 2382 (1984); Phys. Rev. B **33**, 2444 (1988).

[13]G. Gruner, A. Zawadowski, and P. M. Chaikin, Phys. Rev. Lett. **46**, 511 (1981).